JOURNAL OF MAGNETIC RESONANCE **134,** 308–314 (1998)
ARTICLE NO. MN981499

Improved Estimation of CSA–Dipolar Coupling Cross-Correlation Rates from Laboratory-Frame Relaxation Experiments

Ranajeet Ghose[1] and James H. Prestegard[2]

Department of Chemistry, Yale University, New Haven, Connecticut 06520

Received December 2, 1997; revised March 24, 1998

We have investigated the underlying assumptions in estimating cross-correlation rates between chemical shift anisotropy (CSA) and dipolar coupling mechanisms in a scalar-coupled two-spin IS system, from laboratory frame relaxation experiments. It has been shown that for an arbitrary relaxation delay, the difference in relaxation rates of the individual components of an in-phase (or antiphase) doublet is not related to the CSA–dipolar coupling cross-correlation rate in a simple way. This is especially true in the case where the difference in the decay rates of the in-phase and antiphase terms of the density matrix becomes comparable to the magnitude of the scalar coupling between the two spins. Improved means of extracting cross-correlation rates in these cases are presented.

Key Words: **relaxation; cross-correlation; chemical shift anisotropy; dipolar coupling; laboratory frame relaxation rates.**

INTRODUCTION

Cross-correlation between chemical shift anisotropy (CSA) and dipolar coupling can cause differential line broadening in a scalar-coupled IS spin system (*1*). An accurate quantitation of this phenomenon, in a case where the dipolar interaction is known in solution, offers a measure of the CSA of a given nucleus (or, more accurately, the projection of the CSA on the internuclear vector involved in the dipolar interaction). This fact has been utilized by several investigators to measure the CSA of amide ^{15}N (*2*), amide ^{1}H (*3, 4*), and $^{13}C_{\alpha}$ (*5*) in proteins. The magnitude of the CSA in the latter two cases has been shown to be correlated with secondary structure and the hydrogen bonding environment of the nucleus in question. Thus, a measure of the CSA of a given nucleus provides a powerful tool to probe local structural effects in biomolecules. This interference effect has also been used to study local anisotropic motion involving nuclei of the peptide backbone (*6*). It is thus imperative that an accurate quantification of this phenomenon be obtained. Most of the experiments commonly applied to estimate the cross-correlation rates between CSA and dipolar coupling rely on measuring the rate of buildup of antiphase magnetization from in-phase magnetization (or vice versa) associated with a doublet in the laboratory frame (*2–5*). Usually, several assumptions are made to simplify the dynamics of the spin system, allowing extraction of cross-correlation rates from such experiments. The intent of this paper is to explicitly state and examine the validity of these assumptions and propose more accurate means of extracting cross-correlation rates.

THEORY

Most laboratory frame experiments to measure cross-correlation between CSA and dipolar coupling rely on the fact that if one starts with a density operator given by I_y, at the beginning of a relaxation period 2τ, differential relaxation of the two lines of the doublet, represented by $\frac{1}{2}(I_y \pm 2I_yS_z)$, will cause a buildup of $2I_yS_z$ at the end of the period. The ratio of the expectation values of the $2I_yS_z$ and the I_y components of the density matrix may then be used to estimate the cross-correlation rate. To obtain insight into the behavior of the various components of the density matrix during the course of such an experiment, let us consider the spin dynamics during the pulse sequence element depicted in Fig. 1. The initial density matrix $\sigma(0)$ is given by I_y. The time evolution of the density matrix is given by the solution to the Liouville–von Neumann equation (*7, 8*), in the following way:

$$\sigma(t) = \exp(-Lt)\sigma(0). \quad [1]$$

Here $\sigma(0)$ is the initial density matrix and $\sigma(t)$, that after time t. The density matrix may be written as a linear combination of orthonormal spin operators in Liouville space (*7, 8*), which in the case of a scalar coupled two-spin *IS* system is 16-dimensional. In our case we may restrict our attention to that part of the Liouville space spanned by the operators I_y, $2I_xS_z$, I_x, $2I_yS_z$. In this reduced space, the Liouvillian supermatrix $L = -i\mathcal{H} + \Gamma$, during the τ periods (where $\mathcal{H}$ and Γ are the Hamiltonian and relaxation superoperators, respectively), may be approximated by

[1] Present address: Université de Lausanne, Section de Chimie, BCH, CH 1015, Lausanne-Dorigny, Switzerland.

[2] To whom all correspondence should be addressed at Complex Carbohydrate Research Center, University of Georgia, 220 Riverbend Road, Athens, GA 30602-4712.

1090-7807/98 $25.00

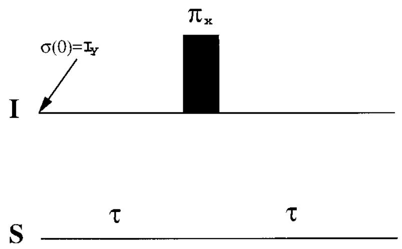

FIG. 1. The basic pulse sequence element used in most laboratory frame experiments to measure interference effects in relaxation due to cross-correlation between CSA and dipolar coupling.

$$L = \begin{bmatrix} R_i & \pi J & 0 & \eta \\ -\pi J & R_a & \eta & 0 \\ 0 & \eta & R_i & -\pi J \\ \eta & 0 & \pi J & R_a \end{bmatrix} \qquad [2]$$

Here, R_i and R_a are the relaxation rates of the in-phase and antiphase components, respectively, J is the coupling constant, and η is the relaxation contribution from the cross-correlation between the CSA of spin I and the IS dipolar coupling. In this approximation, we have neglected the effects of chemical shift evolution during the two τ periods. However, if we choose to observe the system only after the period 2τ, the chemical shift evolution would have been refocused by the π pulse. Moreover, chemical shift evolution during the τ periods interconverts the terms I_x and I_y ($2I_xS_z$ and $2I_yS_z$), which relax equivalently. Hence, [2] is adequate for our purposes.

It is possible to obtain exact analytical solutions for the density matrix at the end of the 2τ period, but this is very algebraically tedious, so we will make a few approximations and investigate the validity of these approximations. Let us consider the limit where η is much smaller than both R_i and R_a, which is often true. In this case, we may set $\eta = 0$ in [2], allowing us to focus on that part of the Liouville space that is spanned by the operators I_y and $2I_xS_z$. This two-dimensional subspace is, in the absence of cross-correlation effects, "decoupled" from that part of Liouville space spanned by the I_x and $2I_yS_z$ terms. The expression for the density matrix at the end of the 2τ period may be expressed as (*9*)

$$\begin{aligned} \sigma(2\tau) &= I_y\left[\left(\frac{2\pi J}{C}\right)^2 - \frac{\Delta R}{C}\left(\frac{\Delta R}{C}\cos(C\tau) - \sin(C\tau)\right)\right] \\ &\quad \times \exp(-R_{av}2\tau) - 2I_xS_z\,\frac{\Delta R}{C}\frac{2\pi J}{C} \\ &\quad \times [1 - \cos(C\tau)]\exp(-R_{av}2\tau), \end{aligned} \qquad [3]$$

where $R_{av} = \frac{1}{2}(R_i + R_a)$, $\Delta R = R_a - R_i$, and C is given by

$$C = \sqrt{(2\pi J)^2 - (\Delta R)^2}. \qquad [4]$$

In the limit where $2\pi J \gg \Delta R$, we have $C \approx 2\pi J$ and $\Delta R/C \approx \Delta R/2\pi J \ll 1$. Neglecting terms higher than first-order in $\Delta R/C$, we may rewrite [3] as

$$\sigma(2\tau) = I_y\left[1 + \frac{\Delta R}{2\pi J}\sin(2\pi J\tau)\right]\exp(-R_{av}2\tau). \qquad [5]$$

Another approximate approach to obtaining an expression for the density matrix at the end of the 2τ period is to average the relaxation superoperator Γ over the various terms of the density operator weighted by the time spent as each of the terms, in analogy to average Hamiltonian theory (*10–12*). Thus, the I_y term observable at the end of the 2τ period may be assumed to relax monoexponentially with an average relaxation rate R_i', which is a weighted average of R_i and R_a with relative weights of $\cos^2(\pi J\tau)$ and $\sin^2(\pi J\tau)$. Integrating this over the 2τ period, we have (*13*)

$$R_i' = R_{av} - \left[\frac{\sin(2\pi J\tau)}{4\pi J\tau}\right]\Delta R. \qquad [6]$$

Thus, neglecting the small off-diagonal terms, the density matrix may be written as

$$\sigma(2\tau) = I_y\exp(-R_i'2\tau). \qquad [7]$$

In the limit where $2\pi J \gg \Delta R$, expanding [7] in a power series and neglecting terms higher than first-order, we have

$$\sigma(2\tau) = I_y\left[1 + \frac{\Delta R}{2\pi J}\sin(2\pi J\tau)\right]\exp(-R_{av}2\tau), \qquad [8]$$

which is identical to the expression derived in the previous paragraph, i.e., [5].

We will now reintroduce cross-correlation effects while working in the $2\pi J \gg \Delta R$ limit of the average Liouvillian formula, presented in the previous paragraph. We further assume that $2\pi J \gg \eta$; this allows us to work in the Liouville subspace of dimension 2 spanned by the operators I_y and $2I_yS_z$ (or, equivalently, $2I_xS_z$ and I_x). The Liouvillian in this case is given by

$$L = \begin{bmatrix} R_i' & \eta \\ \eta & R_a' \end{bmatrix}, \qquad [9]$$

where the R_i' is the average in-phase relaxation rate given by [6] and R_a' is the average antiphase relaxation rate given by

$$R_a' = R_{av} + \left[\frac{\sin(2\pi J\tau)}{4\pi J\tau}\right]\Delta R. \qquad [10]$$

Diagonalizing the Liouvillian of [9], we obtain the eigenvalues

$$\lambda_\pm = R_{av} \pm \frac{1}{2}\sqrt{\left[\frac{\sin(2\pi J\tau)}{2\pi J\tau}\,\Delta R\right]^2 + (2\eta)^2}. \qquad [11]$$

The eigenvectors of [9] are proportional to $I^\pm = \frac{1}{2}(I_y \pm 2I_yS_z)$, which are the two components of the in-phase doublet, and $\lambda_\pm$ correspond to the relaxation rates of $I^\pm$. Thus, if one starts with an initial density operator $\sigma(0) = I_y$, the expectation values of the relevant parts of the density operator, i.e., the expectation values of I_y and $2I_yS_z$ at the end the 2τ period, are given by

$$\langle I_y\rangle(2\tau) = \frac{1}{2}\left[1 - \left(\frac{\frac{\sin(2\pi J\tau)}{2\pi J\tau}\,\Delta R}{\lambda_+ - \lambda_-}\right)\exp(-\lambda_- 2\tau) + \left(1 + \frac{\frac{\sin(2\pi J\tau)}{2\pi J\tau}\,\Delta R}{\lambda_+ - \lambda_-}\right)\exp(-\lambda_+ 2\tau)\right] \qquad [12]$$

and

$$\langle 2I_yS_z\rangle(2\tau) = -\frac{\eta}{\lambda_+ - \lambda_-}[\exp(-\lambda_- 2\tau) - \exp(-\lambda_+ 2\tau)]. \qquad [13]$$

In most laboratory frame determinations of the cross-correlation rates, two experiments are collected. In the first experiment, the expectation value $\langle 2I_yS_z\rangle(2\tau)$ is determined, and in the second one, the expectation value $\langle I_y\rangle(2\tau)$ is determined. The ratio of the expectation values, S, is then analyzed to extract a value of η. In principle, the ratio of [12] to [13] can be plotted for various values of ΔR and η and fit to experimental data to extract the relevant parameters. We will use this as one approach in what follows.

A more common assumption is that S can be given as follows (*2*):

$$S = \frac{\langle 2I_yS_z\rangle(2\tau)}{\langle I_y\rangle(2\tau)} = -\tanh(2\eta\tau). \qquad [14]$$

It is evident from [12] and [13] that even at the approximate level of these equations, [14] holds only in the limit where $[\sin(2\pi J\tau)/(2\pi J\tau)]\Delta R$ is very small, i.e., when the in-phase and antiphase terms do not have significantly different decay rates, making $\Delta R \approx 0$; or when $\Delta R \ll 2\pi J$, or when $\tau \gg 1/J$. In an isolated two-spin system, the decay rates of the in-phase and antiphase terms are equal in the slow-tumbling limit (*14*). However, spins are seldom isolated and ΔR is rarely close to zero. For example, if I is an amide ^{15}N, and S is an amide proton (which has homonuclear interactions with several other protons), the antiphase term decays much faster than the in-phase term. The decay rate of the antiphase term may, in this case, be represented as the sum of the in-phase decay rate and the selective proton longitudinal decay rate (*15*). There is another situation where [14] would hold; this is when $2\eta \gg \Delta R$. However, this is not usually realizable in real systems. It should be stated here that satisfying either of the two conditions just stated, i.e., $[\sin(2\pi J\tau)/(2\pi J\tau)]\Delta R$ is very small or $2\eta \gg \delta R$, is sufficient for [14] to hold. This is the case in the situations considered in Refs. (*2–6*).

Although departures from [14] are to be expected when we depart from the limit $\Delta R \ll 2\pi J$, inspection of [6], [10], and [11] reveals that a simplification takes place at particular values of τ. When $2\tau = n/J$, and n is an integer, $R'_i = R'_a = R_{av}$, and [11] transforms to

$$\lambda_\pm = R_{av} \pm \eta, \qquad [15]$$

Substituting [15] into [12] and [13], we obtain exactly [14]. This suggests that there may be some advantage in a judicious choice of τ values. The other limit where [14] holds true is when $\tau \gg 1/J$, i.e., when the relaxation delay is long enough to allow many oscillations between in-phase and antiphase terms, thus allowing the in-phase and antiphase components of the Liouville space to be sampled equally. In that case the $\sin(2\pi J\tau)/(4\pi J\tau)$ term in [6] and [10] is very small and can be neglected. As a result, we again have $R'_i = R'_a = R_{av}$. Operation in this limit may be somewhat impractical because of the loss of signal at very long τ.

SIMULATIONS AND DISCUSSION

We have simulated the effects of cross-correlation in a two-spin IS system. Simulations were performed using three levels of theory; the exact calculations using the numerical diagonalization of [2] (henceforth referred to as method I), the average Liouvillian approach using the analytical expressions in [12] and [13] (referred to as method II), and finally the direct calculation of signal intensity using [14] (called method III). The numerical matrix manipulations were performed using the subroutines of the CLAPACK library (*16*), available from Netlib. All calculations were performed on a Silicon Graphics INDY (R4400) workstation.

Figures 2a–2c depict the ratio of the expectation values of $2I_yS_z$ and I_y at the end of the 2τ period calculated using the three different methods mentioned above. The R_i, R_a, and η values used in the calculations were 6.0, 12.0, and 4.0 s^{-1}, respectively. The J values used were 3.0 Hz (2a), 6.0 Hz (2b), and 24.0 Hz (2c). It is seen from Fig. 2a that for small values of $2\pi J$, when the limit $2\pi J \gg \Delta R$ is not satisfied, III (dot-dashed curve) produces a value for the ratio of the expectation values which is very different from that obtained from both the exact calculation (I) (solid curve) and the average Liouvillian approach (II) (dotted curve). The latter two values seem to agree quite well except for very large values of the relaxation

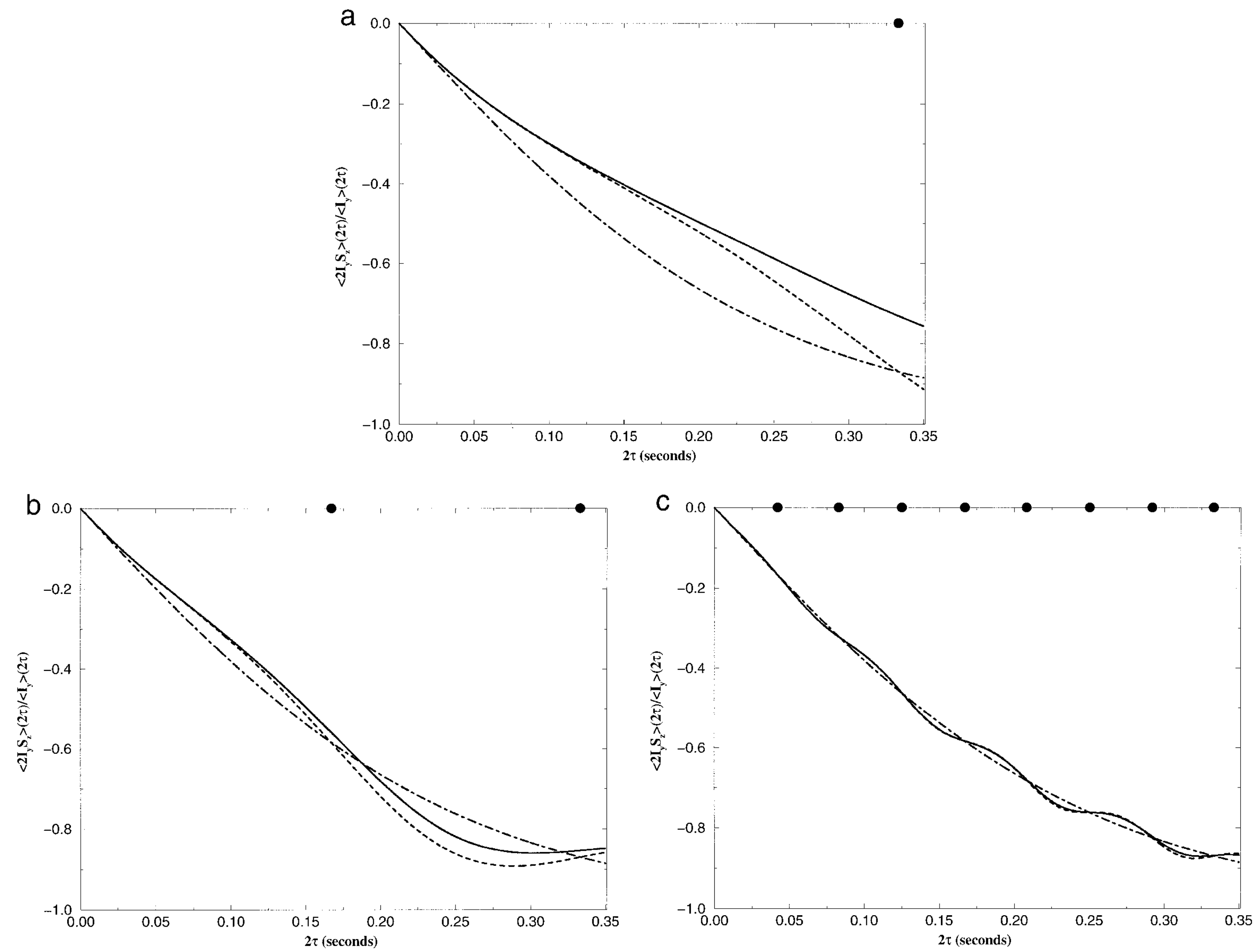

FIG. 2. The value of $\langle 2I_yS_z\rangle(2\tau)/\langle I_y\rangle(2\tau)$ as function of the relaxation delay, 2τ. The values of the coupling constant, J, used are 3.0 Hz (a), 6.0 Hz (b), and 24.0 Hz (c). The solid line represents the curve calculated using method I, the dotted line is that calculated using method II, and the dot-dashed line has been calculated using III. The 2τ values which correspond to n/J ($n = 1, 2, \ldots$) have been indicated by circles.

period 2τ, even though in this limit, the equivalence of [3] and [7] is no longer valid, and the average Liouvillian approximation (II) no longer holds. For larger values of $2\pi J$, the ratio as determined by the exact calculation (I) (solid curve) and that determined using the average Liouvillian (II) (dotted curve) oscillate about the value obtained by using [14], the commonly applied approximation (III) (dot-dashed curve). The crossing of the two curves determined using methods I and III occurs at 2τ values alternating between slightly greater and slightly less than multiples of $1/J$. In the case of the average Liouville approach (II), the curves (II and III) cross at 2τ values which are exact multiples of $1/J$, as expected from [12] and [13].

Inspection of [12] and [13] suggests the source of oscillation as coming principally from the $\langle I_y\rangle(2\tau)$ term, whereas the $\langle 2I_yS_z\rangle(2\tau)$ shows no significant oscillations. The oscillations in $\langle I_y\rangle(2\tau)$ are oscillations of the spin-echo amplitude as shown by Meersmann and Bodenhausen (*9*). The oscillatory behavior of the two terms can be understood by realizing that the two terms constituting [12] and [13] have similar oscillatory behavior. This is reinforced in [12] due to the + sign and reduced in [13] due to the − sign.

Figures 3a–3c depict the magnitude of the deviation of the exact value of S from that calculated using the average Liouvillian approach (solid curve) (II) and that calculated using [14] (III) (dotted curve). Represented are rms deviations as a percentage of the signal obtained using method I. The deviation can be quite large in the case where one deviates from the $2\pi J \gg \Delta R$ limit for the calculation using [14] (III), but this deviation decreases with an increase in 2τ as shown by the dotted curves in Fig. 3). The deviations in the average Liouvillian case (II) tend to be small at small values of 2τ and increase with increasing 2τ (solid curve in Fig. 3), but on an average they never reach the deviations displayed for method III.

Both curves undergo periodic zero crossings. In both cases

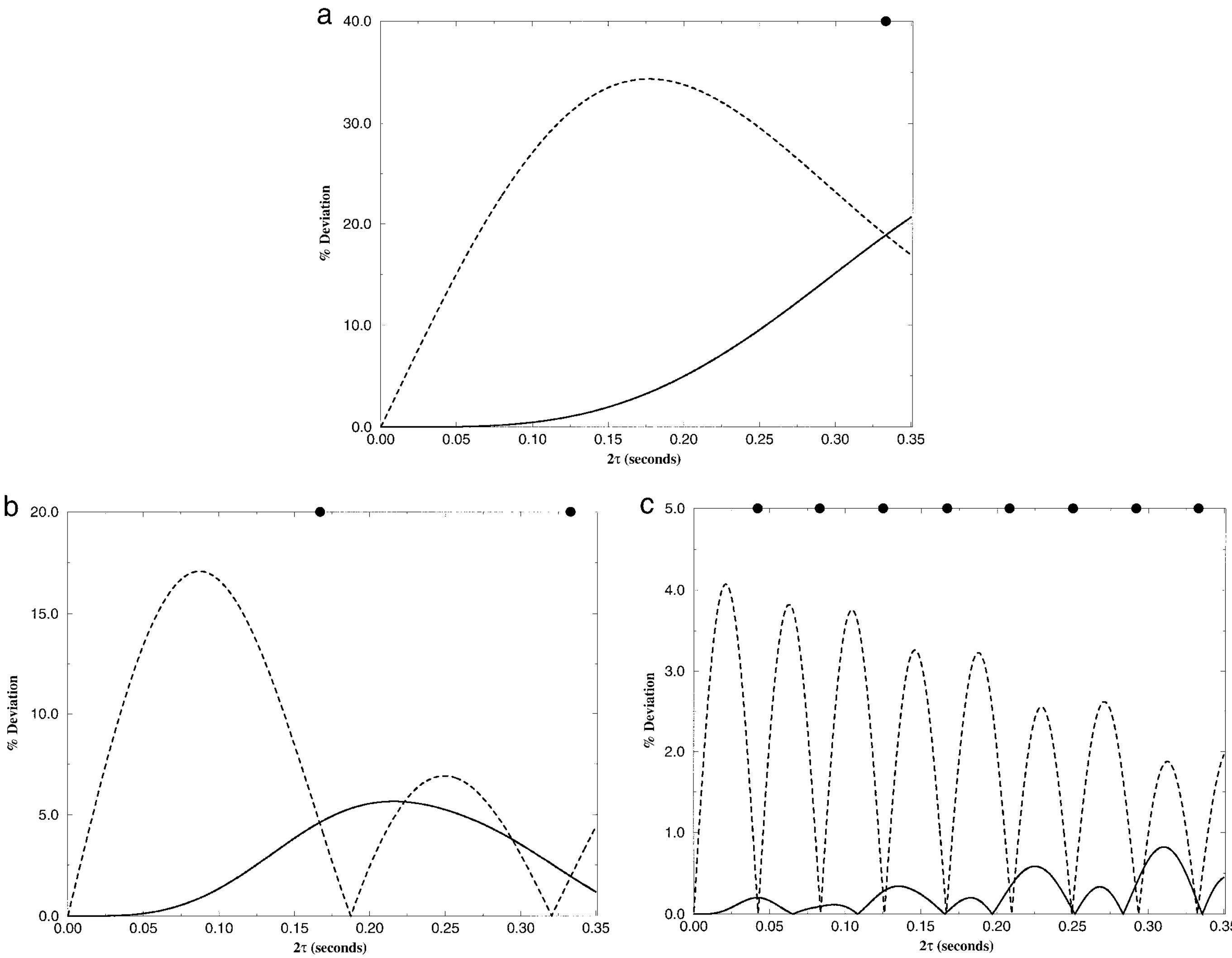

FIG. 3. The root mean square deviation of $\langle 2I_yS_z\rangle(2\tau)/\langle I_y\rangle(2\tau)$ for the methods II (solid curve) and III (dotted curve) from that obtained from the exact calculation (I), as a percentage of the signal obtained from the exact calculation (I), plotted as a function of the relaxation time 2τ. The 2τ values which correspond to n/J ($n = 1, 2, \ldots$) have been indicated by circles.

zero crossings occur at times which are slightly larger than multiples of $1/J$ (after the last zero crossing) for odd-numbered zero crossings, and slightly smaller than multiples of $1/J$ for even-numbered zero crossings, after the first one or two zero crossings. Initially, the curves calculated using the Liouvillian approach (II) (solid curve) tend to intersect with those calculated using the exact approach (I) at times which are slightly longer than the times at which the curves calculated using [14] (dotted curve) cross the exact curves, for odd-numbered intersections. The situation is reversed for even-numbered intersections, where the crossings of the curves generated using methods (I) and (II) occur at times which are shorter than the corresponding crossing times of the curves produced using methods (III) and (I). At moderately large values of 2τ, the zero crossings converge to similar time points (see Fig. 3c). Thus, it may be said that in the case where the magnitude of $2\pi J$ is comparable to ΔR, the results produced by both the average Liouvillian approach (II) and [14] (III) deviate from those predicted by the exact theory. However, the deviation in the former case is generally smaller than the latter case; it is significantly smaller when the value of 2τ is small. It can thus be said that the average Liouvillian approach produces better agreement with the exact calculation at short τ values. It must be stated here (as pointed out by one of the reviewers) that in the limit $\eta \gg 2\pi J$, method II is no longer a better description of the real situation than method III. However, cases where this limit holds are rare in real situations.

Finally, we consider the effects of using [14] (the most commonly utilized method) to estimate the value of η at two different values of J (6.0 and 24.0 Hz) at a ΔR value of 6.0 s^{-1}. We have generated relaxation curves using the exact theory (I), and then extracted the value of η using [14]. The results are

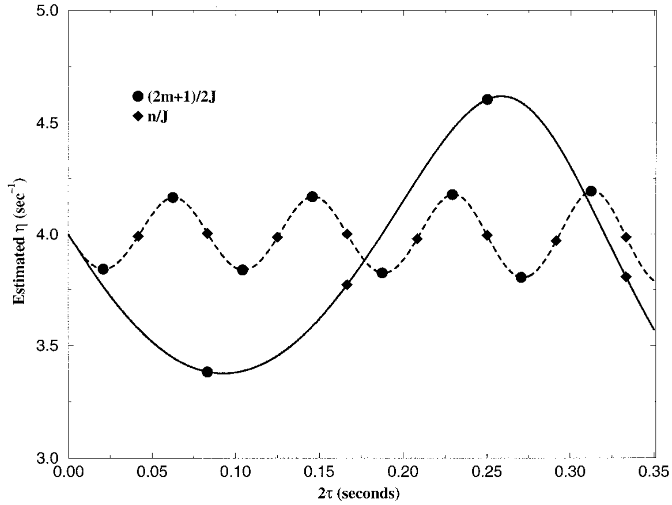

FIG. 4. Values of η estimated using an inversion of [14] for $J = 6.0$ Hz (solid curve) and $J = 24.0$ Hz (dashed curve). The correct value of η is 4.0 s^{-1}. The 2τ which correspond to n/J ($n = 1, 2, \ldots$) and $(2m + 1)/2J$ ($m = 0, 1, 2, \ldots$) are represented by circles and diamonds, respectively. Note that the latter are distributed to the two sides of the true value of η, at alternate points.

shown in Fig. 4. The correct value of $\eta = 4.0\ s^{-1}$. Using [14] to estimate η would yield erroneous results at values of 2τ which are quite different from multiples of $1/J$. This is especially true when $2\pi J$ values are comparable to ΔR, as can be seen from the solid curve ($J = 6.0$ Hz, $\Delta R = 6.0\ s^{-1}$) in Fig. 4. However, we see that making two sets of measurements at 2τ values of $(2m + 1)/2J$ ($m = 0, 1, 2, \ldots$) at two successive values of m (this is where the deviation from the correct value is the largest) and then averaging the two values yields the correct value of η because of cancellation of errors. This value is even more accurate than picking a value of 2τ which is a multiple of $1/J$. As is evident from the solid line in Fig. 4 ($J = 6.0$ Hz), using the value of η at $2\tau = 1/J$ and $2\tau = 2/J$ yields values of η which are 3.77 and 3.80. Taking the average between the values of η at $2\tau = 1/2J$ (3.38) and $2\tau = 3/2J$ (4.60) gives a value of 3.99 which is very close to the correct value of 4.0. When $2\pi J \gg \Delta R$ ($J = 24.0$ Hz, $\Delta R = 6.0\ s^{-1}$, dashed line in Fig. 4), both methods produce results which are similar and close to the correct value of η.

CONCLUSIONS

In conclusion, calculation of cross-correlation rate constants (η) between CSA and dipolar coupling in two-spin systems can be pursued by making simplifying assumptions about spin-relaxation contributions and deriving expressions for the time course of the ratio of the expectation values of the in-phase and antiphase components of the signal. An average relaxation approach provides a modest improvement over the most commonly employed set of assumptions, especially for measurements that must be made with small coupling constants and short relaxation periods (2τ). However, the more common approach, which leads to a simple $\tanh(2\eta\tau)$ dependence on η, can yield good results with a judicious choice of 2τ values. The effects of errors introduced by simplifying assumptions can be largely avoided by choosing certain values of the relaxation delay 2τ equal to $(2m + 1)/2J$ ($m = 0, 1, 2, \ldots$) for two successive values of m (e.g., $2\tau = 1/2J$ and $2\tau = 3/2J$). The success of this method would rely on some preliminary knowledge of the values of the coupling constants J. Additionally, if some estimate of the various relaxation rates, i.e., R_a, R_i, and η, are available, it would allow one to decide whether it would be sufficient to use [14] to obtain an accurate estimate of η, or whether a more sophisticated analysis would be required. We have chosen the experiments of (*2*) as an example of experiments which rely on representing the decay rates of the lines of scalar-coupled doublets as $R_{av} \pm \eta$. The same arguments could apply to other experiments which make similar assumptions (*4*).

ACKNOWLEDGMENT

This work has been supported by a grant GM 33225 from the National Institutes of Health.

REFERENCES

1. M. Goldman, Interference effects in the relaxation of a pair of unlike spin-$\frac{1}{2}$ nuclei, *J. Magn. Reson.* **60,** 437–452 (1984).

2. N. Tjandra, A. Szabo, and A. Bax, Protein backbone dynamics and ^{15}N chemical shift anisotropy from quantitative measurement of relaxation interference effects, *J. Am. Chem. Soc.* **118,** 6986–6991 (1996).

3. N. Tjandra and A. Bax, Solution NMR measurement of amide proton chemical shift anisotropy in ^{15}N-enriched proteins. Correlation with hydrogen bond length, *J. Am. Chem. Soc.* **119,** 8076–8082 (1997).

4. M. Tessari, H. Vis, R. Boelens, R. Kaptein, and G. W. Vuister, Quantitative measurement of relaxation interference effects between $^{1}H_N$ CSA and ^{1}H–^{15}N dipolar interaction: Correlation with secondary structure, *J. Am. Chem. Soc.* **119,** 8985–8990 (1997).

5. N. Tjandra and A. Bax, Large variations in $^{13}C^{\alpha}$ chemical shift anisotropy in proteins correlate with secondary structure, *J. Am. Chem. Soc.* **119,** 9576–9577 (1997).

6. M. W. F. Fischer, L. Zeng, Y. Pang, W. Hu, A. Majumdar, and E. R. P. Zuiderweg, Experimental characterization of models for backbone pico-second dynamics in proteins. Quantification of NMR auto- and cross-correlation relaxation mechanisms involving different nuclei of the peptide plane, *J. Am. Chem. Soc.* **119,** 12629–12642 (1997).

7. R. R. Ernst, G. Bodenhausen, and A. Wokaun, “Principles of Nuclear Magnetic Resonance in One and Two Dimensions,” Clarendon Press, Oxford (1987).

8. J. Cavanagh, W. J. Fairbrother, A. Palmer III, and N. J. Skelton, “Protein NMR Spectroscopy Principles and Practice,” Academic Press, San Diego (1996).

9. T. Meersmann and G. Bodenhausen, Relaxation-induced oscillations of spin-echo envelopes, *Chem. Phys. Lett.* **257,** 374–380 (1996).

10. U. Haeberlen, "Advances in Magnetic Resonance," Suppl. 1, Academic Press, San Diego (1976).

11. J. Briand and R. R. Ernst, Sensitivity comparison of two-dimensional correlation spectroscopy in the laboratory frame and in the rotating frame, *J. Magn. Reson. A* **104,** 54–62 (1993).

12. B. C. Gerstein and C. R. Dybowski, "Transient Techniques in NMR of Solids," Academic Press, San Diego (1985).

13. A. Palmer III, N. J. Skelton, W. J. Chazin, P. E. Wright, and M. Rance, *Molec. Phys.* **75,** 699–711 (1992).

14. J. Peng and G. Wagner, Protein mobility from multiple ^{15}N relaxation parameters, *in* "Nuclear Magnetic Resonance Probes of Molecular Dynamics" (R. Tycko, Ed.), pp. 373–449, Kluwer Academic Publishers, Dordrecht (1994).

15. L. E. Kay, L. K. Nicholson, F. Delaglio, A. Bax, and D. A. Torchia, Pulse sequences for removal of the effects of cross-correlation between dipolar and chemical shift anisotropy relaxation mechanisms on the measurement of heteronuclear T_1 and T_2 values in proteins, *J. Magn. Reson.* **97,** 359–375 (1992).

16. CLAPACK is the C version of the matrix manipulation library LAPACK available from http://www.netlib.org/clapack.